

Selective Excitation of Higher-radial-order Laguerre-Gaussian Beams Using a Solid-state Digital Laser

Bell T^{1,2*} and Ngcobo S¹

¹Council for Scientific and Industrial Research, PO Box 395, Pretoria, 0001, South Africa
²University of KwaZulu-Natal, Private Bag X 54001, Durban 4000, South Africa

Abstract

In this paper, we use a digital laser to generate high-radial-order Laguerre-Gaussian, LG $p,0$ modes by loading digital holograms on a phase-only spatial light modulator that act as an end mirror of a diode-end-pumped laser resonator. The digital holograms were encoded with an amplitude ring mask, which contained absorption rings that match the p -zeros of the Laguerre polynomial. We demonstrate the generation of high-quality LG $p,0$ modes with a mode volume that is directly proportional to the mode order, p . This work demonstrates the possible of using the digital laser as a tool for simulating optical elements that will be used in pursuing high brightness lasers.

Keywords: Lasers; Laser resonators; Spatial light modulators; Holographic optical elements; Laser beam shaping; Laser beam characterization

Introduction

Since high power solid-state lasers are the most developing branches of laser science and they have become an increasingly important tool for modern technology inside the end pumped solid-state laser resonator [1]. A new design of these solid-state lasers in a form of a digital laser was recently discovered by South African researchers [2]. This technology may lead into a new era in laser manufacturing and their applications in the industry where this digital laser will be used as simulation [3] and testing tool [4,5] in many future laser manufacturing processes. The solid-state digital laser is pumped using a diode laser, due to better frequency stability, higher efficiency, higher brightness and long operational lifetime that is provided by diode lasers [6]. The digital laser comprises of an intra-cavity phase-only spatial light modulator (SLM) that acts as an end mirror of the laser resonator cavity. The SLM is used to introduce a phase mask and/or amplitude mask inside the laser resonator by digitally loading a grey-scale hologram image that represents a mask of interest. The digital laser is limited in the output power it can produce, when compared to standard diode-end-pumped solid-state lasers [7-9] due to low damage threshold of the SLM. Nevertheless, the digital laser is found to be a stable intra-cavity beam shaping tool, which can be used to simulate any desired intra-cavity optical element prior to it being manufactured. In this paper we show how to generate high-radial-order Laguerre-Gaussian (LG $p,0$) modes from zero up a radial order, $p=3$, by selectively encoding and loading amplitude digital holograms mask on a phase-only SLM that contain absorbing rings that match the p -zeros of the Laguerre polynomial. We show that the generated LG $p,0$ modes results are very consistent with similar previous [10] experimental results there were obtained using a physical diffractive optical element that was lithographically engraved with aluminium absorbing rings and inserted inside the resonator cavity. We show that the results obtained in this paper are far more superior because of the better design of the amplitude mask that allows for better mode matching of the laser the pump and the absorbing rings.

Radial Laguerre-Gaussian Modes

The electric field of Radial Laguerre-Gaussian modes, LG $p,0$, where p is the radial order geometries can be mathematically represented by the following equation:

$$\mu_{p,0} = \sqrt{\frac{2}{\pi}} \times \frac{1}{w} \times L_p^0 \left(\frac{2r^2}{w^2} \right) \times e^{-\frac{r^2}{w^2} - \frac{ikr^2}{2R(z)}} \times e^{-i(2p+1)\arctan\left(\frac{z}{R}\right)} \quad (1)$$

Where r is the radial coordinates, and L_0 is the Laguerre polynomial. All other parameters have their usual meaning [9,11]. LG $p,0$ consist of central peak that surrounded by p concentric rings. The Laguerre polynomial ($L_p(X)$, letting $X=2r^2/w^2$) for the rings is define in Table 1.

The spot size w is to only define the fundamental Gaussian beam, LG $0,0$ where the radial order, p , equals to zero. For higher-radial-order Laguerre-Gaussian, LG $p,0$, modes their intensity profiles consist of a central peak that is surrounded by p concentric rings of light and dark rings. The intensity profile of the dark concentric rings of the (LG $p,0$) modes matches the Laguerre polynomial p -zeros. The intensity profile of the LG $p,0$ modes is defined by the absolute square of Eq. 1 and the LG $p,0$ beam

Width, w_p , which is based on a second moment radius is given as:

$$w_p = w\sqrt{2p+1} \quad (2)$$

and the propagation factor, M^2 , of such modes is given as:

$$M_p^2 = 2_p + 1 \quad (3)$$

To force the laser to generate LG $p,0$ modes, a mask containing p absorbing rings that have a geometry which closely follows the location

p	$L_p(X)$
0	1
1	1-X
2	$X^2/2 - 2X + 1$
3	$-X^3/6 + 3X/2 - 3X + 1$

Table 1: Laguerre Polynomials.

***Corresponding author:** Bell T, Council for Scientific and Industrial Research, Council for Scientific and Industrial Research, Pretoria, GP, South Africa, Tel: +27 31 260 8596; E-mail: tbell@csir.co.za

Received November 28, 2016; **Accepted** December 02, 2016; **Published** December 30, 2016

Citation: Bell T, Ngcobo S (2016) Selective Excitation of Higher-radial-order Laguerre-Gaussian Beams Using a Solid-state Digital Laser. J Laser Opt Photonics 3: 144. doi: 10.4172/2469-410X.1000144

Copyright: © 2016 Bell T, et al. This is an open-access article distributed under the terms of the Creative Commons Attribution License, which permits unrestricted use, distribution, and reproduction in any medium, provided the original author and source are credited.

of the Laguerre Polynomial p -zeros as illustrated in Table 2 [12], were digitally encoded to the SLM of the digital laser [2], which will then allow for the generations of such $LG_{p,0}$ modes.

Experimental Methodology and Concept

To generate radial-order Laguerre-Gaussian, $LG_{p,0}$ modes we consider a planoconcave solid-state digital laser resonator that is end-pumped with a multi-mode fibre coupled diode laser, where the Hamamatsu spatial light modulator (SLM 1) is encoded with an amplitude mask that will function as an end mirror of the resonator. The amplitude mask is encoded to have p absorbing rings of varying width thickness that will 80% match each null of the $LG_{p,0}$ mode, for radial-order $p=1-3$. A schematic of the experimental setup is presented in Figure 1.

The gain medium Nd:YAG rod crystal (4 mm × 25 mm) had a 1.1% neodymium concentration and was anti-reflection coated for 808 nm to minimise pump reflections. The laser crystal was mounted inside a 21°C water-cooled copper block. The pump diode laser (Jenoptik, JOLD-75-CPXF-2P) had a maximum output power of 75 Watts at an emission wavelength of 808 nm (at an operating temperature of 25°C). The pump diode laser output was coupled into a fibre with a core diameter of 400 μm and was fast axis collimated and a lens coupled to end-pump the Nd:YAG crystal by using a 25.4 mm (L1) and 150 mm (L2) focal length spherical lenses, respectively. A gain area with a diameter of 2 mm was then excited within the centre of the Nd:YAG rod crystal. The planoconcave cavity comprised of a phase-only spatial light modulator (SLM 1) (Hamamatsu) which acted as an end mirror of the cavity with a reflectivity of 95% and a curved output coupler mirror with a radius of curvature of 400 mm and a reflectivity of 90%. The resonator was designed to form a Z-shape (in order to avoid illuminating the SLM with the residual pump light) by including a

p	r_j/w			
0	0.707106			
1	0.541195	1.306562		
2	0.455946	1.071046	1.773407	
3	0.401589	0.934280	1.506090	2.167379

Table 2: Roots of Laguerre polynomials.

45° mirrors (M2) within the cavity that were highly reflective for 1064 nm and highly transmissive for 808 nm. The resonator length was chosen to be 173 mm and the Nd:YAG crystal centre was positioned 120 mm from the SLM 1 [2]. The Line Filter (LF) was introduced to only transmit 1064 nm and block the 808 nm pump. The laser beam was transmitted out of the cavity through an output coupler mirror (M3 on Figure 1) and was 1:1 relay imaged using two 125 mm lenses (L3 and L4) to a Photon ModeScan Meter for measuring the beam quality factor M^2 . The emitted beam was also 1:1 relay imaged using two 125 mm lenses (L3 and L5) to the Meadowlark optics spatial light modulator (SLM 2) to perform modal decomposition [13,14] into the Laguerre-Gaussian basis and the measurement of signal at the origin of the Fourier plane using a 125 mm lens (L6) was captured using a CCD camera (Spiricon, LBA-USB).

Numerical Simulations

We perform a numerical calculation of the fundamental mode of the resonator that will contain an intra-cavity amplitude mask. The simulation is based on the expansion of the resonant field on the basis of the eigenmodes of the bare cavity (without any diffracting object). This method will not be given here since it has been already described elsewhere for the case of a Plano-concave cavity including an absorbing ring on the plane mirror [12]. The modelling gave in ref. [12] can be easily adapted to the case of an amplitude mask made up of concentric absorbing rings just by evaluating the overlapping integral (Eq. A10 of Ref. [12]) upon all the regions of transparency of the mask. The width of the absorbing rings is simulated to be a 98% match of the $LG_{p,0}$ mode p -zero nulls that will be oscillating inside the resonator. This allows for better mode selection since each absorbing ring width will be tailor designed to match the oscillating $LG_{p,0}$ mode p -zero nulls inside the resonator as shown in Figure 2. The simulated $LG_{p,0}$ modes of $p=1-3$ cross-section profiles are shown in Figure 2. The thickness of the absorbing rings for the $p=3$ mode increases from the inner ring to the outer ring. The minimum thickness of the ring is 20 μm which corresponds to the pixel pitch of the SLM 1.

Experimental Results and Discussion

The results of selectively generating $LG_{p,0}$ modes with an

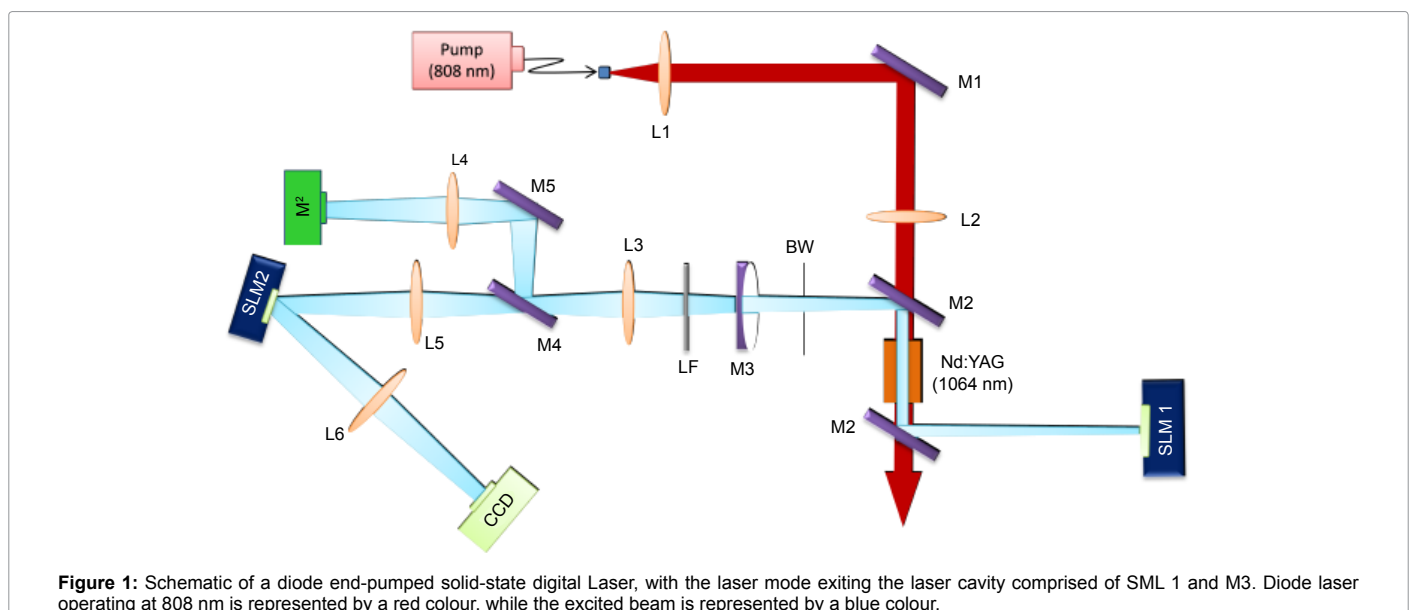


Figure 1: Schematic of a diode end-pumped solid-state digital Laser, with the laser mode exiting the laser cavity comprised of SML 1 and M3. Diode laser operating at 808 nm is represented by a red colour, while the excited beam is represented by a blue colour.

appropriate grey scale masks that contain absorbing rings are shown in Figure 3. The grey scale images in Figure 3a-3d which are also termed the digital holograms that contains absorbing rings and aperture, were encoded on the SLM using complex amplitude modulation [15] The laser beam profiles of the generated LG_{p,0} modes in Figure 3.

3 (e-h) clearly match the corresponding grey scale digital holograms. This is what we were expecting for the generated LG single modes of orders $p=0-3$. It is also clear that in Figure 3e-3h the width of the p -zero intensity nulls on the generated LG_{p,0} modes increases as the order of the mode increases, which allows for better mode matching with the encoded digital hologram absorbing rings. Since the generated high-order LG_{p,0} modes come from a stable resonator cavity, their beam radius, w , and beam propagation factor, M^2 , of the modes are known analytically, they can be compared to experimental results as there are summarised in Figure 4a. It is evident that the cavity is selecting desired modes with appropriate beam sizes and beam propagation factors which are all in good agreement with the theory. It is evident that the cavity is selecting desired modes with appropriate beam sizes and beam propagation factors which are all in good agreement with the theory. Furthermore, the modal decomposition [13] was performed to determine the mode purity of the generated high-order LG_{p,0} modes. In Figure 4b the mode purity is greater than 90% for modes $p=0$ and $p=2$, and then dropping to just below 95% to 90% for $p=1$ and $p=3$

respectively. The output power from a laser is defined to be linearly proportional to the mode volume, V_p , where the volume of the p th radial mode is found from:

$$\begin{aligned} V_p &= \int_0^{l_0} \pi w^2(z) dz \\ &= \pi w_0^2 (2p+1) \left(1 + \frac{l_0^2}{3z_r^2} \right) \\ &= v_o M^2 \left(1 + \frac{l_0^2}{3z_r^2} \right) \end{aligned} \quad (4)$$

Where l_0 is the length of the gain medium and V_0 is the mode volume of the $p=0$ (Gaussian) mode (Figure 4).

In the limit that the length of the crystal is much smaller than the Rayleigh range of the beam, then Eq. 4 simplifies to $V_p = M^2 V_0$. The results of the output power versus input power for the LG_{0,0} mode and LG_{3,0} mode are shown in Figure 5a. The results for slope efficiency and pump power threshold (Figure 5) of the generated LG_{p,0} modes of $p=0-3$ are shown in Figure 5b. The digital aperture in Figure 3a-3d was encoded because we wanted to minimize the losses, an increased number of transverse modes will go below a certain loss threshold required to maintain a steady-state oscillation, and selectively excite required LG_{p,0}. Since the beam radius is proportional to Eq. 2, it is a reasonable assumption that the diffraction losses of the LG_{p,0} mode will exhibit the highest slopes if the aperture radius is varied around a value of about $\times 4$ the Gaussian beam radius. The threshold pump power show in Figure 5b, indicated by a blue solid line is required to reach a gain factor G of more than 1.0, for modes to be excited. The detailed knowledge of the diffraction losses of the transverse modes is crucial for the optimized design of a laser resonator, especially for lasers with low gain media. The pump power required to reach threshold is determined by the losses the radiation experiences in a round trip. The gain factor per transit G_0 has to compensate the losses generated by output coupling and diffraction. The threshold condition reads as follow:

$$G_0 \geq \frac{1}{\sqrt{R_1 R_2} V} \quad (5)$$

Where R_1 and R_2 are the reflectance of SLM 1 and mirror M3, and V is loss factor per round trip. In addition, the efficiency of a laser is heavily affected by internal losses in the laser resonator. The output power is also inversely proportional to the round-trip losses. This suggests that the higher-order radial modes have an output power that may be expressed by Eq. 6, this is evident from Figure 5b:

$$\frac{P_p}{P_0} = (2p+1) \times \frac{\sigma_0}{\sigma_p} \quad (6)$$

where the subscripts p and 0 refer to the radial mode orders and the round trip losses are denoted by σ . It is clear that higher order modes extract more power compared to mode order of $p=0$, this is due to an increase in mode volume, as shown by Eq. 4. This will be possible if the round trip losses can be kept to a minimum compared to the extracted gain, as shown by Eq. 6. This is evident in Figure 5a that shows a graph of the output power versus input power of the LG_{0,0} and LG_{3,0} modes. At the input power (P_{in}) of above 18.2 W, the power extracted from LG_{p,0} mode of order $p=3$ exceeds that of the fundamental Gaussian mode, $p=0$, by a factor of 1.2, despite the fact that the LG_{3,0} mode have a higher loss. This is because the extra gain compensates for the extra losses when the laser resonator generates the LG_{3,0} mode. These results show that it is possible to select a higher-order LG_{p,0} mode of the very high beam quality factor and mode purity, with an aim of extracting

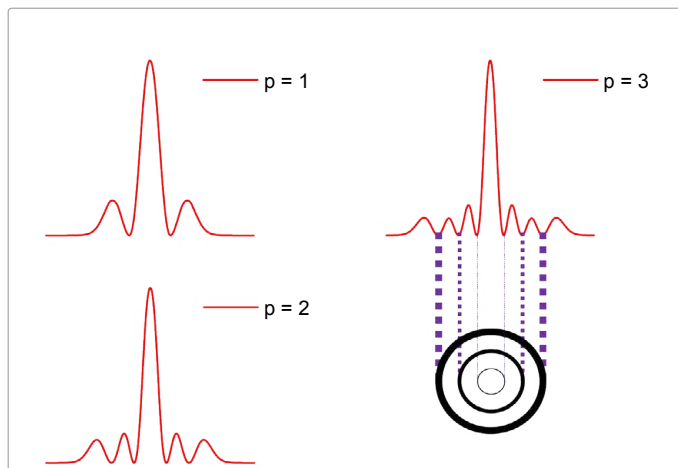


Figure 2: Intensity cross section of numerically simulated lowest-loss eigenmodes for $p=1$ to 3 when a mask containing an absorbing p rings is inserted inside the resonator. The mask is inserted such that the high-loss absorbing rings coincide with the intensity p -zero nulls for an example for $p=3$ Laguerre-Gaussian mode.

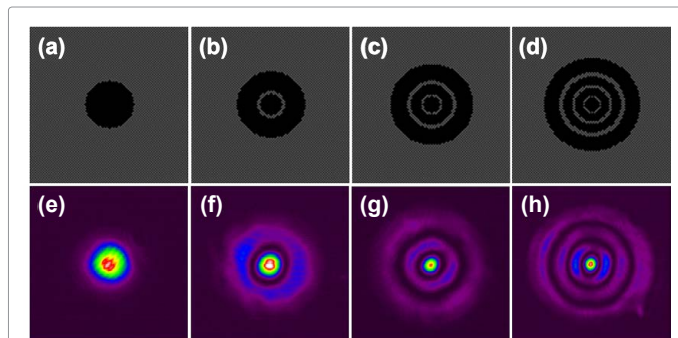


Figure 3: Observed intensity profiles of the Laguerre-Gaussian of order, $p=0-3$, at the output coupler. (a)-(d) Gray scale holograms with amplitude modulation in form of checkerboard. (e)-(h) Intensity profiles.

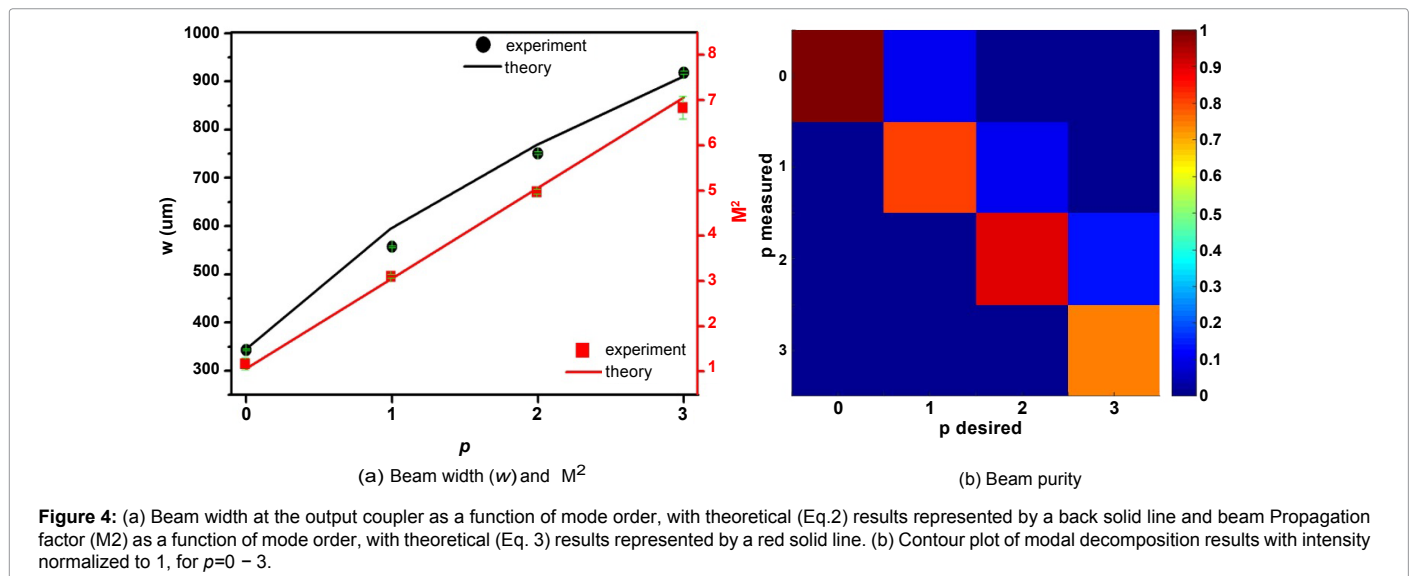


Figure 4: (a) Beam width at the output coupler as a function of mode order, with theoretical (Eq.2) results represented by a back solid line and beam Propagation factor (M^2) as a function of mode order, with theoretical (Eq. 3) results represented by a red solid line. (b) Contour plot of modal decomposition results with intensity normalized to 1, for $p=0-3$.

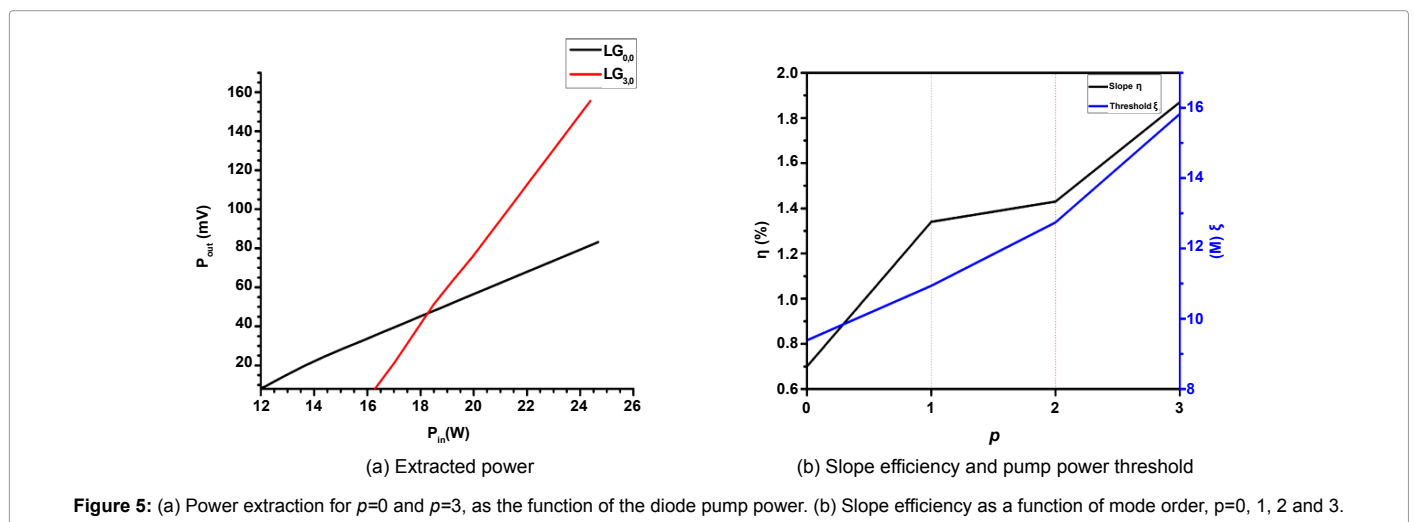


Figure 5: (a) Power extraction for $p=0$ and $p=3$, as the function of the diode pump power. (b) Slope efficiency as a function of mode order, $p=0, 1, 2$ and 3 .

more power within a laser resonator that contains an intra-cavity SLM encoded with amplitude absorbing rings mask that operates as an end mirror of the resonator.

Conclusion

We have shown that it is possible to selectively excite high radial order LG modes of $p=0-3$, which are in very good agreement with the theoretically expected results for the beam profiles, sizes and quality factor. Our results show that one can digitally excite a single high order $\text{LG}_{p,0}$ mode, by loading a grey-scale digital hologram that represents the mode of interest with an aim of extracting more power from the laser gain medium. We have shown that generating an $\text{LG}_{3,0}$ mode, we can extract more power from the digital laser gain medium than generating the lowest order, $\text{LG}_{0,0}$, mode when using an amplitude mask that is introduced on intra-cavity SLM that acts an end mirror of the resonator. Our results suggest that a digital laser can be used as a simulation test tool for manufacturing amplitude masks for the development of the high-brightness laser that will operate by selective excitation of a single higher-order $\text{LG}_{p,0}$ laser modes above the critical input power.

Acknowledgements

This work is based on the research supported by the National Research Foundation (NRF), Republic of South Africa (RSA).

Funding: National Research Foundation (NRF) (PDP2014).

References

1. Poprawe R (2014) Ultrafast lasers with kW class output power for applications in industry and science. Opt Soci Ameri pp: AM1A-2.
2. Ngcobo S, Litvin I, Burger L, Forbes A (2013) A digital laser for on-demand laser modes. Nat Commun 4: 2289.
3. Ngcobo S, Ait-Ameur K, Litvin I, Hasnaoui A, Forbes A (2013) Tuneable Gaussian to flat-top resonator by amplitude beam shaping. Opt express 21: 21113-21118.
4. Litvin IA, Ngcobo S, Naidoo D, Ait-Ameur K, Forbes A (2014) Doughnut laser beam as an incoherent superposition of two petal beams. Opt lett 39: 704-707.
5. Ngcobo S, Bell T, Litvin IA, Naidoo D, Ait-Ameur K, et al. (2015) Selective excitation and detection of higher-order doughnut laser modes as an incoherent superposition of two petals modes in a digital laser resonator. Int Society Opt Photo pp: 95810B-95810B.
6. Bru'ning R, Ngcobo S, Duparr'e M, Forbes A (2015) Direct fiber excitation with a digitally controlled solid state laser source. Opt lett 40: 435-438.

7. Fan TY, Byer RL (1988) Diode laser-pumped solid-state lasers. Science 24: 895-912.
8. Koehner W (2006) Solid-State Laser Engineering. Optical resonator. Springer.
9. Hodgson W (2005) Laser resonators and beam propagation. Springer Series Optical Sciences 451: 500.
10. Ngcobo S, Ait-Ameur K, Passilly N, Hasnaoui A, Forbes A (2013) Exciting higher-order radial Laguerre-Gaussian modes in a diode-pumped solid-state laser resonator Appl Opt 52: 2093-2101.
11. Shimoda K (2013) Introduction to laser physics. Springer.
12. Hasnaoui A, Ait-Ameur K, (2010) Properties of a laser cavity containing an absorbing ring. Appl Opt 49: 4034-4043.
13. Flamm D, Naidoo D, Schulze C, Forbes A, Duparré M (2012) Mode analysis with a spatial light modulator as a correlation filter. Opt lett 37: 2478-2480.
14. Schulze C, Ngcobo S, Duparre M, Forbes A (2012) Modal decomposition without a priori scale information. Opt express 20: 27866-27873.
15. Arrizon V, Ruiz U, Carrada R, Gonzalez LA (2007) Pixelated phase computer holograms for the accurate encoding of scalar complex fields. JOSA A 24: 3500-3507.

Citation: Bell T, Ngcobo S (2016) Selective Excitation of Higher-radial-order Laguerre-Gaussian Beams Using a Solid-state Digital Laser. J Laser Opt Photonics 3: 144. doi: [10.4172/2469-410X.1000144](https://doi.org/10.4172/2469-410X.1000144)

OMICS International: Open Access Publication Benefits & Features

Unique features:

- Increased global visibility of articles through worldwide distribution and indexing
- Showcasing recent research output in a timely and updated manner
- Special issues on the current trends of scientific research

Special features:

- 700+ Open Access Journals
- 50,000+ editorial team
- Rapid review process
- Quality and quick editorial, review and publication processing
- Indexing at major indexing services
- Sharing Option: Social Networking Enabled
- Authors, Reviewers and Editors rewarded with online Scientific Credits
- Better discount for your subsequent articles

Submit your manuscript at: <http://www.omicsonline.org/submission>